A New Approach for Designing and Analysis of High Flat Gain Broadband Low Noise Amplifier Using Real Frequency Technique

Reham Magdy[1], Gehan S. Shehata[2], Ahmed S. I. Amar[3], M. ElHawary[1], and Mahmoud A. Mohanna [4]
[1] National Institute for Standards (NIS), Giza, Egypt
[2] Faculty of Engineering, Benha University, Egypt
[3] Electronics and Communications Engineering, Ain Shams University, Egypt
[4] National Research Institute of Astronomy and Geophysics (NRIAG), Egypt
Email: rehammagdy271@yahoo.com; gehan.mohamed@feng.bu.edu.eg; ahmed.s.i.amar@ieee.org; mohamed.ibrahim@nis.sci.eg; mahmoud2746@nrig.sci.eg

***Abstract*—**This paper introduces a high flat gain broadband Low Noise Amplifier (LNA) design approach, which is based on using a new methodology of Real Frequency Technique (RFT). To get this done, the optimum matching network has been designed with second-order LC lumped elements to minimize the Noise Figure (NF) and maximize the Transducer Gain (GT) based on selecting the optimum (Z_S, Z_L) LNA terminations that have been used over a 2.1-4.2 GHz. The design has demonstrated a high stable gain in the range of 19.19 –18.73 dB with ± 0.2 dB gain flatness over the specified band. Moreover, the NF has been obtained at 0.68 – 0.82 dB and a stable operation throughout a broad bandwidth. Furthermore, the proposed method results have been compared with an analytical methodology which is based on computing equivalent input and output circuits for the transistor model using its scattering parameters. For the verification purpose, the performances of the synthesized amplifier are compared using MATLAB platform and ADS simulation software. The output results have a good agreement with the proposed method outcomes, which makes this method a new promising technique for the high flat gain broadband LNA design.

***Index Terms*—**Broadband matching networks, LNA, RFT, analytical broadband matching

I. Introduction

With the growth of communication systems such as modern wireless devices that support various air interface technologies, like 3G, 4G, and 5G, the requirement for high sensitivity, high-speed transmissions, and broadband networks is steadily increasing [1], [2]. On the other hand, broadband topology affects noise performance [3], [4]; consequently, researchers have performed considerable progress in designing broadband Low Noise Amplifiers (LNAs) for different frequency bands mainly used on the receiving side. Therefore, they play a crucial role in the noise performance and sensitivity of the whole receiver chain. Basically, the broadband LNA has a unique design that meets several strict requirements, such as low Noise Figure (NF), flat gain, good input matching, and adequate stability [5].

Designing broadband or wideband matching networks is highly desirable, and it is also necessary to obtain gain flatness and low NF [6]. The Smith Chart, a traditional method for impedance matching, is an effective tool to match a single working frequency [7]. Generally, to expand bandwidth and obtain a high flat gain and low NF level, the broadband LNA matching networks require several elements, which unavoidably increase the parasitic losses. However, for multi-bands, high-performance LNAs are highly required. Many design methodologies for LNAs have been published [8], like the resistive shunt feedback topology [9], distributed topology [10], and multi-stage cascaded amplifiers (common gate-common source) topology [11]. Although design methodologies vary depending on the topology employed, some design specifications always have to be considered, as indicated above. The research has recently focused on designing broadband power amplifiers using numerical (RFT) or analytical methods [12], [13]. RFT is a wideband semi-analytic design method to realize lossless matching networks with optimum circuit topologies. Besides, this approach has been successfully demonstrated in the design of broadband power amplifiers with bandwidths of more than 63% [14]. Meanwhile, it's worth noting that practical broadband matching networks have been designed and carried on using the low pass ladder structure as lossless LC, which has been one of the most practical topologies for broadband matching and is commonly introduced for simplicity in synthesis and physical construction. However, according to our survey, many researchers have not applied RFT to design broadband LNA that achieves high flat gain and maintains Low NF.

Our target is to demonstrate a high flat gain broadband LNA design with the numerical method by modified RFT that achieved high gain flatness and maintained a minimum NF. Subsequent comparison with an analytical approach in the frequency spectrum from 2.1 to 4.2 GHz has been performed in order to validate the agreement between the outcomes. The proposed work has been

Manuscript received August 15, 2021; revised February 1, 2022.
Corresponding author email: van.nguyenngoc@hust.edu.vn.
doi:10.12720/jcm.17.10.777-785

arranged in the upcoming sections. Section II shows biasing method and stability circuit for the active device using ADS simulation. Furthermore, in this section, steps for synthesizing matching networks using RFT and analytical methods have been shown. The simulation results for gain and NF over the selected band for both methods are listed in Section III. Finally, in Section IV, the conclusion of this research has been reported.

II. Circuit Analysis and Design

The design steps of the proposed LNA are shown in this section below. Here, we prefer not to use the pre-mentioned traditional techniques because it's our target to focus on using general design broadband matching network handling techniques. Furthermore, the simplicity of the broadband single-stage LNA is illustrated in Fig. 1. It can be categorized into three parts: The Input Matching Network (IMN), the Output Matching Network (OMN), and the DC bias circuit. The proposed design is analyzed by MATLAB codes, simulated, and optimized with Advanced Design System (ADS).

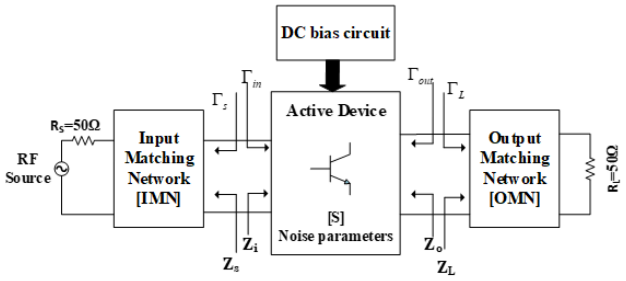

Fig. 1. Simplified illustration of the proposed broadband LNA.

A. Bias Setting and Stabilize the Active Device

In the design process, the discrete BFU730f device of NXP Company was selected for different reasons. Some of the main selection criteria are; being cost-effective and having a wide range of applications in a plethora of electronic circuits. It is DC-biased and appropriately adjusted to operate in Class A operating mode, with a collector voltage VCE= 2 V and a base current IBB = 50 µA, providing with a collector current IC= 17 mA, according to the datasheet biasing conditions [15].

Following the selected DC bias, Stability analysis is among the most important considerations to avoid the active device oscillation and to show the optimum amplifier performance. Equations (1) and (2) demonstrate that the amplifier's stability criteria are fulfilled.

$$K=\frac{1-|s_{11}|^2-|s_{22}|^2+|\Delta|^2}{2|s_{12}s_{21}|}>1. \quad (1)$$

$$|\Delta|=s_{11}s_{22}-s_{12}s_{21}<1. \quad (2)$$

where K is the stability factor, Δ is the determinant of [s], [s] is the scattering parameters of the selected BFU730f device within the operating range.

Obviously, the stability factor (K) for the selected BFU730f within the desired frequency range hasn't met the pre-selected condition elucidated in equation (1). In order to tackle the stability problems, instead of using graphical analysis to determine the regions in the Smith chart that produces a stable amplifier with the values of (Z_S, Z_L), another method has been used. In order to maintain the NF as low as possible, the active's output port has been loaded with an appropriate resistor [16]. By applying this procedure, parallel RC as a stability circuit has been designed such that R_{stab}=303 Ω and C_{stab}=1.5 µF. The simulated stability parameters from ADS software depicted in Fig. 2 demonstrate that the designed circuit has achieved the stability criteria (K>1) and ($|\Delta|<1$) within the selected operating band.

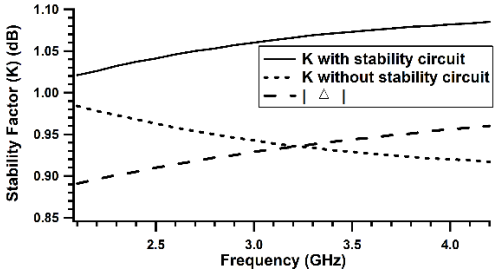

Fig. 2. Simulated stability factor (K) with and without designed stability circuit.

B. Optimum (Z_S, Z_L) Extraction for RFT

IMN and OMN are defined in terms of their associated impedances and calculated at discrete frequency points. Using the Smith chart analysis tool, the stability, noise, and gain circles have been plotted in Fig. 3 in order to extract the optimum Z_S and Z_L. Because of the added stability circuit, the input stability circles have been positioned around the Smith chart's border. The locus of optimum source impedances on the Smith chart is a trade-off between gain and noise figure. Therefore, it was a challenge to select the optimum impedances that could achieve the required performance. First and foremost, the optimum source impedance is determined for the minimum noise figure, maximum gain, as an example, at the frequency point of 2.1 GHz, a trade-off is made by choosing the point where the NF =0.69 dB noise circle intersects with the GA = 22.58 dB available gain circle. Γ_s=0.171+j0.051 and $Z_S=(44.058+j7.591)\Omega$ are the values in this illustration. Equation (3) is used to calculate the output reflection coefficient for the selected Γ_s. In order to obtain the lowest output VSWR, the load reflection coefficient, which is the complex conjugate of the output reflection coefficient, has to be calculated using $\Gamma_L=\Gamma_{out}^*$, Γ_L=0.071+j0.261 and $Z_L=(55.118+j23.792)\Omega$.

$$\Gamma_{out}=S_{22}+\frac{S_{12}S_{21}\Gamma_s}{1-S_{11}\Gamma_s}. \quad (3)$$

The stated procedure has been performed for frequencies ranging from 2.1 to 4.2 GHz with step size 0.1 GHz to evaluate the frequency-dependent behavior of the input and output matching networks.

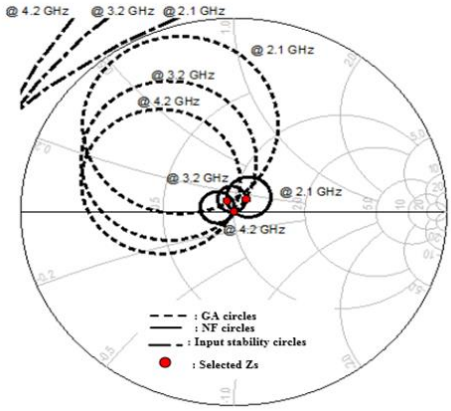

Fig. 3. Available gain, noise, stability circles for selecting optimum Z_S at 2.1, 3.2, 4.2 GHz.

C. Synthesis of the Impedance Matching Networks

The design of IMN and OMN using the RFT method is a particular case of a lossless Matching Network [MN] in terms of its Positive Real (PR) driving point input impedance function $Z_2(j\omega)$. Synthesis of broadband matching networks, that have different configurations, is based on a low pass, high pass, and band pass structure. In many practical cases, it is not preferable to introduce finite transmission zeros in the matching network. And hence, it is more common that the matching network is designed as a low pass LC structure [17] as illustrated in Fig. 4. The proposed approach is analyzed using a two-order low pass circuit for IMN and OMN to achieve the best noise figure and gain while preserving broadband bandwidth.

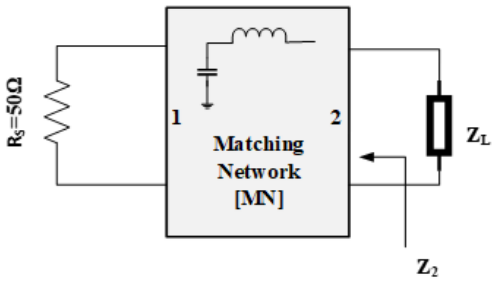

Fig. 4. Representation of the lumped elements matching network.

The lumped elements of matching networks can be constructed by the rational form of the driving point impedance $Z_2(s)=N(s)/D(s)$; $s=(j\omega)$, which can be expressed as $Z_2(j\omega)=R_2(\omega)+jX_2(\omega)$ and can be obtained by optimizing the transducer power gain TPG as shown in equation (4) [12].

$$TPG(\omega)=\frac{4* R_2(\omega)* R_L(\omega)}{\left[R_2(\omega)+R_L(\omega)\right]^2+\left[X_2(\omega)+X_L(\omega)\right]^2} \quad (4)$$

where $Z_L(j\omega)=R_L(\omega)+jX_L(\omega)$ is the load data that has been obtained from the active device and calculated by the optimum (Z_S, Z_L). The matching issue aims to maximize TPG while maintaining NF as low as possible at the input matching network. TPG is maximized by choosing a flat gain level T_0 under reactance cancellation.

The driving point impedance for passive elements network is assumed to have a minimum reactance impedance; as a result, it may be calculated uniquely from its non-negative real part $R_2(\omega)$ that can be used to calculate the imaginary part $X_2(\omega)$ using Hilbert transformation relation as well. The optimal value $R_2(\omega)$ is determined by a least-squared nonlinear optimization algorithm to minimize the error function in equation (5) for pre-fixed gain level T_0 as high and flat as possible over the specified range.

$$Error_{TPG,\,n}(\omega)=\sum_{i=1}^{M}\left[TPG(\omega_i,X)-T_0\right]^2 \quad (5)$$

where vector X represents the load data $Z_L(\omega)$ and all breakpoints $R_0(\omega)$; the idealized form of $R_2(\omega)$. Here the realistic implementation condition of a matching network can be expressed as $Re\{Z_2(s)\}>0$; where $Re\{Z_2(s)\}$ should be even rational function as indicated in equation (6) [18].

$$R_2(\omega^2)=\frac{a_0^2\omega^{2ndc}\prod_{i=1}^{nz}(\omega_i^2-\omega^2)^2}{B_1\omega^{2n}+B_2\omega^{2(n-1)}+\cdots+B_n\omega^2+1} \doteq \frac{A(\omega^2)}{B(\omega^2)}\geq 0\,.\forall\omega\,. \quad (6)$$

where ndc is the order of transmission zeros at DC, nz is the total number of transmission zeros, ω_i is finite transmission zeros on the $j\omega$ axis. In the low pass case, ndc is set to zero, $\prod_{i=1}^{nz}(\omega_i^2-\omega^2)^2$ is set to 1, and hence $A(\omega^2)$ equals to a_0^2; the Real constant a_0 is linked to selecting an ideal transformer in the matching network. The transformer is not included in the chosen circuit, so a_0 is set to 1. To achieve a minimum impedance function $Z_2(s)$, The denominator coefficients of the real part have to be positive and real. Therefore, the denominator has to be represented as $B(\omega^2)=\frac{1}{2}\left(c^2(\omega)-c^2(-\omega)\right)$; where $c(\omega)$ is an arbitrary polynomial with real coefficients are determined by the designer using ad-hoc initialization. Equation (6) is transformed to a rational form where all the parameters of the minimum immittance function in the Bode form are characterized by:

$$F_B(p)=F_0+\sum_{i=1}^{n}\frac{k_i}{p-p_i}. \quad (7)$$

$$F_0=\frac{A_1}{B_1}\geq 0. \quad (8)$$

$$k_i=(-1)^n\frac{A(p_i^2)}{p_iB_1\prod_{j=1,i\neq j}^{n}(p_i^2-p_j^2)},\ j=1,2,\ldots,n. \quad (9)$$

where n is the number of poles and A_1, B_1 are positive real leading coefficients from equation (6), k_i is called the residue of its corresponding pole pi.

Designing IMN with RFT should address low noise considerations by choosing Z_s that has been settled on the proper Noise figure circles [19].

$$\left|\Gamma_s - \frac{\Gamma_{opt}}{1+N_i}\right|^2 = \frac{N_i^2 + N_i\left(1-\left|\Gamma_{opt}\right|^2\right)}{(1+N_i)^2}. \quad (10)$$

$$N_i = \frac{F_i - F_{min}}{4r_n}\left|1+\Gamma_{opt}\right|^2. \quad (11)$$

where N_i is NF parameter for a noise figure F_i, and the values of F_{min}, r_n, Γ_{opt} are known as noise parameters, they are computed at every sample frequency point by producing or by simulating the ADS. After determining Fi from the selected Z_s, the N_i is calculated at each frequency point. Furthermore, RFT included only the error of TPG. Equation (12) has been used to add the noise figure error, which has been minimized by choosing proper Zs.

$$Error_{NF}(\omega) = \left[\left|\Gamma_{s,n} - \frac{\Gamma_{opt}}{1+N_i}\right|^2 - \frac{N_i^2 + N_i\left(1-\left|\Gamma_{opt}\right|^2\right)}{(1+N_i)^2}\right]^2. \quad (12)$$

The sum of errors is defined in the following equation:

$$Error_{TPG,\,NF}(\omega) = \sum_{i=1}^{n}\left[Error_{TPG}(\omega) + Error_{NF}(\omega)\right] \quad (13)$$

It is preferable to avoid the long computation with an early approximation of T_0; for instance, T_0=0.97. The normalized input reflection looking into the equalizer and the optimum Z_S is given by equation (14)

$$\left|S_{in}(j\omega)\right| = \sqrt{1-TF(\omega)}. \quad (14)$$

where TF is the TPG of IMN. The appropriate network is next constructed and simulated by ADS as Fig. 5(a). The results of the MATLAB synthesizer have been checked by comparing with TPG simulated ADS, as illustrated in Fig. 5(b). There is a good agreement between ADS and MATLAB outcomes, indicating that the synthesizer is highly efficient. Return Loss S_{11} obtained from ADS and MATLAB is displayed in Fig. 5(c).

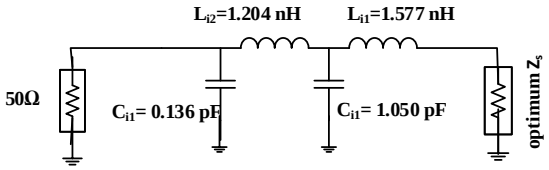

(a)

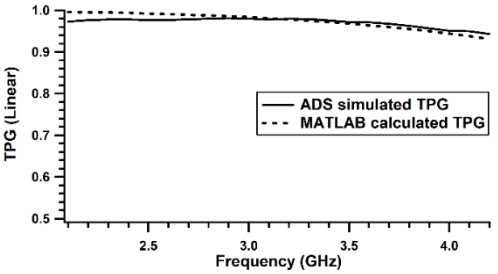

(b)

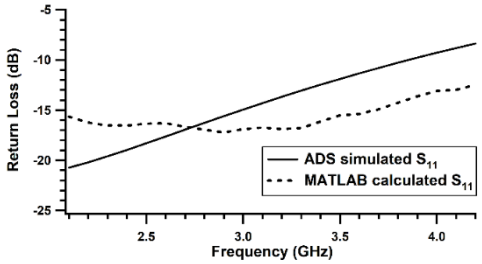

(c)

Fig. 5. Comparison between ADS and MATLAB results (a) lumped elements of the IMN, (b) TPG (Linear) and (c) Return Loss (dB).

The OMN is designed by adjusting the TPG using real frequency data obtained from the selected optimum ZL. Because the approximation of T_0 is desirable, the startup procedure T_0=0.92 is a good starting point. The required OMN has been simulated, as shown in Fig. 6(a). Afterward, MATLAB synthesizer and ADS outputs have been compared as shown in Fig. 6(b) and (c) for TPG and Return Loss.

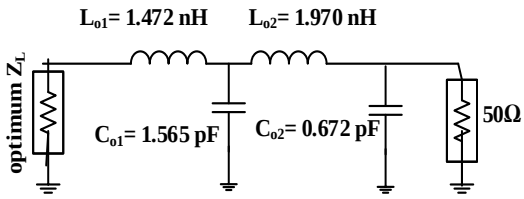

(a)

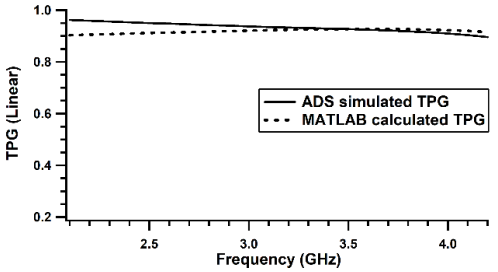

(b)

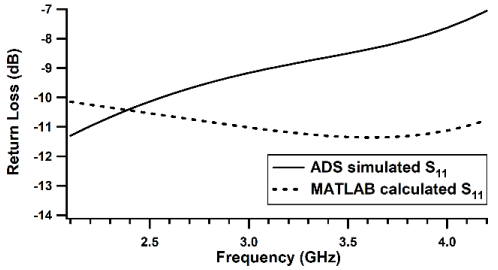

(c)

Fig. 6. (a) lumped elements of the OMN, (b) TPG (Linear) and (c) Return Loss (dB).

The final model is further enhanced using ADS optimization algorithm as depicted in Fig. 7(a). The performance of the proposed prototype LNA has a gain range of 18.733–19.195 dB with ±0.2 dB gain flatness and a great response for NF<1 dB that is demonstrated from 2.1 GHz to 4.2 GHz as indicated in Fig. 7(b) and (c). The element values of the designed matching networks are shown in Table I.

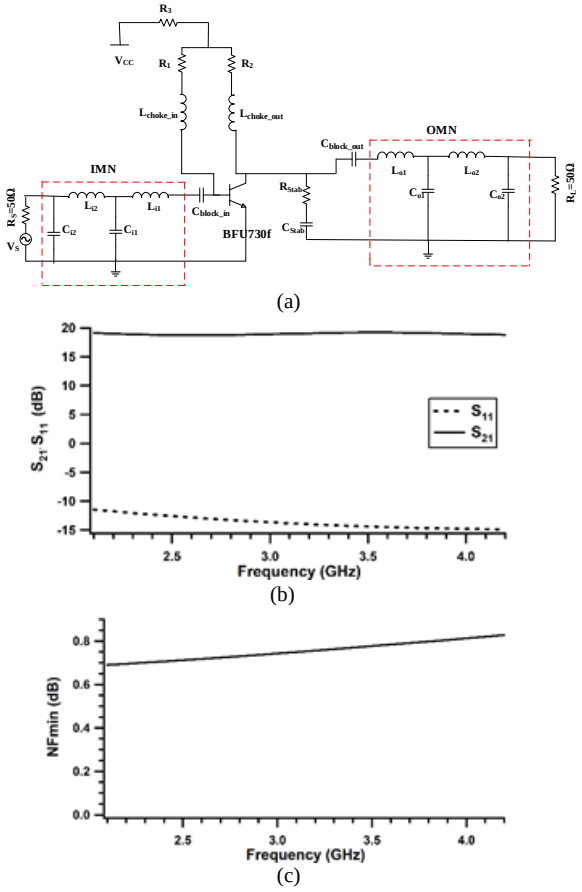

Fig. 7. (a) The proposed designed broadband LNA with RFT, (b) Gain and Return Loss (dB) and (c) NF (dB).

TABLE I: MATCHING ELEMENTS VALUES OF THE PROPOSED BROADBAND LNA

Symbols	L_{i1}(nH)	C_{i1}(pF)	L_{i2}(nH)	C_{i2}(fF)
Values	1.744	1.651	1.007	45.492
Symbols	L_{o1}(nH)	C_{o1}(pF)	L_{o2}(nH)	C_{o2}(fF)
Values	4.335	0.761	2.868	20.084

III. COMPARING THE RESULTS WITH ANALYTICAL METHOD

In this section, a comparison between the proposed RFT as a new approach for designing LNA and the analytical broadband matching theory will be discussed, as indicated in the literature [18], [20]. The mentioned examples have proved that if the analytic theory can solve the matching issue using Chebyshev functions, the solutions achieved using RFT have produced more significant gain responses for a given equalizer complexity. Basically, the roll-off that has occurred for the power gain as frequency increases is around 6 dB/octave. Consequently, a matching circuit is designed to compensate for the roll-off response to obtain a nearly flat broadband response over desired bandwidth. The analytical theory has suggested that the unilateral model can be applied if and only if the transistor is unconditionally stable [21]. Nevertheless, our designed transistor is not stable in the desired range of operation as mentioned above. Hence, in order to be able to use such a model, circuit stability designed above has to be utilized. The measured active device data $Z_L(j\omega)$ used for estimating $Z_2(j\omega)$ of the matching networks can be analyzed with different considerations. $Z_L(j\omega)$ in the numerical method (RFT) relies on the observed optimal loads, whilst in the analytical method depends on the equivalent unilateral model calculated for IMN and OMN at the frequency range of interest. The unilateral simplified circuit model reported in [22] has been used due to its accuracy. The transducer power gain from port 1 to port 2 of [N] is calculated using equation (15).

$$TPG(\omega)=|S_{21}(j\omega)|^2=1-|S_{22}(j\omega)|^2. \quad (15)$$

For $s=j\omega$, $S_{22}(s)$ is given by:

$$S_{22}(s)=\frac{Z_2(s)-Z_L^*(-s)}{Z_2(s)+Z_L(s)}. \quad (16)$$

The poles of $Z_L(-s)$ in $\mathrm{Re}\ s>0$ are the same as that of $S_{22}(s)$. Since the terms $Z_2(s)$ and $Z_L(s)$ are Positive Real (PR), having poles in $\mathrm{Re}\ s>0$ is not desirable. Let $s_i(i=1,2,...m)$ denote the poles of $Z_L(-s)$ (real or complex conjugate pairs). *B*(*s*) can be defined as

$$B(s)=\prod_{i=1}^{n}\frac{s-s_i}{s+s_i}. \quad (17)$$

Then $B(s)$ is an all-pass function that has only poles in $\mathrm{Re}\ s<0$, $B(s)$ is real for real *s* and $B(s)B(-s)=1$. Moreover, the reflection coefficient $\rho(s)$ can be calculated as

$$\rho(s)=B(s)S_{22}(s). \quad (18)$$

Which has only poles in $\mathrm{Re}\ s<0$ by substituting equation (18) in equations (15) and (16), which yields

$$Z_2(s)=\frac{2r_L(s)B(s)}{B(s)-\rho(s)}-Z_L(s). \quad (19)$$

$$r_L(s)=\frac{Z_L(s)+Z_L(-s)}{2}. \quad (20)$$

$$|\rho(j\omega)|^2=1-G(\omega^2). \quad (21)$$

Once $G(\omega^2)$ is defined, $\rho(s)$ can be determined by a spectral factorization due to the analytic continuation property, that is

$$\rho(-s)\rho(s)=1-G(-s^2)=\frac{N(s^2)}{M(s^2)} \quad (22)$$

where $N(s^2)$ and $M(s^2)$ denote the numerator and denominator of $1-G(-s^2)$ respectively. Both of them can be factored as $N(s^2)=n(-s)\,n(s)$, $M(s^2)=m(-s)\,m(s)$, where $n(s)$ and $m(s)$ are formed by the zeros in $\mathrm{Re}\ s<0$. Therefore

$$\rho(s)=\pm\frac{n(s)}{m(s)}. \quad (23)$$

Eventually, for the obtained value of $G(\omega^2)$, $\rho(s)$ can be calculated. Furthermore, if $Z_L(s)$ is given, $Z_2(s)$ can be determined using equation (19). Under certain conditions for $\rho(s)$, $Z_2(s)$ can be analyzed as a passive network [21].

A. Analysis of Equivalent Circuit Models

In the transistor equivalent circuit model, the input can be approximated by a series $R_iL_iC_i$ circuit that is used to estimate the conjugate Γ_m of the optimum noise source reflection coefficient to equalize Γ_m^* and the source impedance R_s (50Ω in practice) in order to get a minimum noise figure. The elements of the input model circuit across 2.1 GHz bandwidth have been computed utilizing MATLAB code, which are $R_i=34.86\,\Omega$, $L_i=0.1$ nH, and $C_i=1.5$ pF. Afterward, $R_iL_iC_i$ has been simulated exploiting ADS software to validate the accuracy of the model. The output can be approximated as shunt-series R_oC_o - L_o as seen in Fig. 8. The output impedance of the proposed model is used to approximate S_{22} of the transistor with a stability circuit. The calculated output circuit elements across a 2.1 GHz bandwidth are $R_o=172.8\,\Omega$, $C_o=0.77$ pF, and $L_o=1.51$ nH. The IMN and OMN are designed based on the pre-calculated Z_i and Z_o as in Fig. 8.

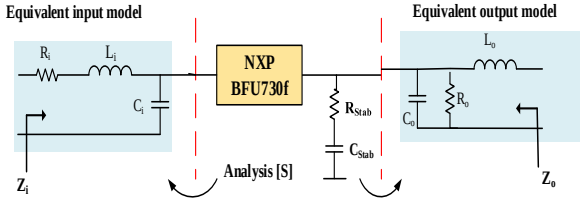

Fig. 8. The equivalent unilateral microwave transistor model.

B. Input Lossless Matching Network

IMN is designed between R_s and the computed input impedance of the transistor Z_i. First of all, slope response of $G(\omega^2)$ with band pass Chebyshev characteristics has been selected to maximize the gain-bandwidth product [21]. In this design, n=2, ε =0.5 and k_2 =1 within the pass band have been chosen in equation (24).

$$G(\omega^2)=\frac{k_2(\omega/\omega_2)^2}{1+\varepsilon^2C_2^2(\omega')}. \quad (24)$$

where ε is ripple factor, k_2 is the pass band gain of $G(\omega^2)$, and $C_n(x)$ is Chebychev polynomial which can be determined by $C_2(\omega')=2\omega'^2-1$, $\omega'=\omega/B-\omega_0^2/B\omega$, $\omega_0^2=\omega_1\omega_2$

where, ω_1 and ω_2 are the lower and upper pass band frequencies. The minimum phase reflection coefficient $\rho(s)$ is calculated through the above steps described using MATLAB code for the pre-mentioned formula.

$$\rho(s)=\frac{s^4+0.321s^3+1.208s^2+0.203s+0.25}{s^4+0.556s^3+1.279s^2+0.278s+0.25}. \quad (25)$$

This $\rho(s)$ for IMN achieves the gain-bandwidth constraints [21]. Under these conditions, $Z_2(s)$ can be synthesized as shown in Fig. 9.

C. Output Lossless Matching Network

OMN that has been positioned between the load R_L and the transistor's equivalent output impedance Z_o is designed, as illustrated in Fig. 1. The low pass type is used for Z_o, and hence the non-sloped response of $G(\omega^2)$ with low pass Chebyshev characteristics has been exploited as elucidated in equation (26) with n=3, ε =0.1.

$$G(\omega^2)=\frac{k_3}{1+\varepsilon^2C_3^2(\omega)}. \quad (26)$$

Substituting for $C_3(\omega)=4\omega^3-3\omega$ the $\rho(s)$ can be obtained as

$$\rho(s)=\frac{s^3+1.209s^2+1.481s+0.68}{s^3+2.348s^2+3.507s+2.5}. \quad (27)$$

Using $\rho(s)$, $Z_2(s)$ can be synthesized in Fig. 9. Next, the calculated IMN and OMN using ADS optimization have been obtained for the broadband LNA. (See Table II)

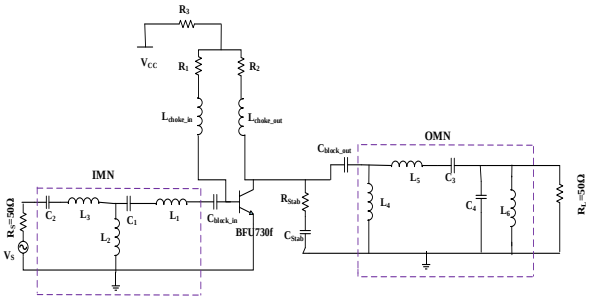

Fig. 9. The proposed designed broadband LNA by analytical method.

TABLE II: THE ELEMENTS VALUES OF THE DESIGNED MATCHING NETWORKS FOR THE PROPOSED BROADBAND LNA BY ANALYTICAL METHOD

Symbols	L_1(nH)	C_1(fF)	L_2(nH)	L_3(nH)	C_2(fF)
Values	3.023	524.5	3.921	3.596	629.4
Symbols	L_4(nH)	L_5(nH)	C_3(pF)	C_4(fF)	L_6(nH)
Values	3.435	0.821	1.074	5	2.655

Fig. 10 shows the proposed LNA performance by the analytical method simulated in Fig. 9. This performance has a gain range of 17.534–18.299 dB with ±0.4 dB gain flatness, and the Noise figure is less than one. There is a good matching between RFT and the Analytical method.

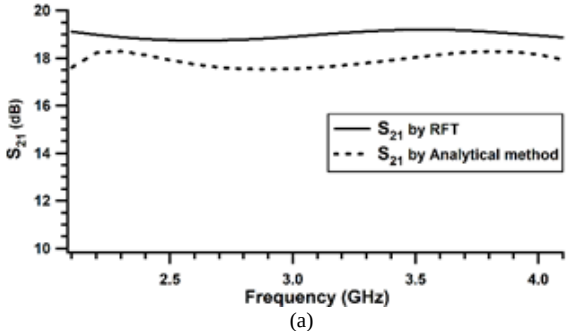

(a)

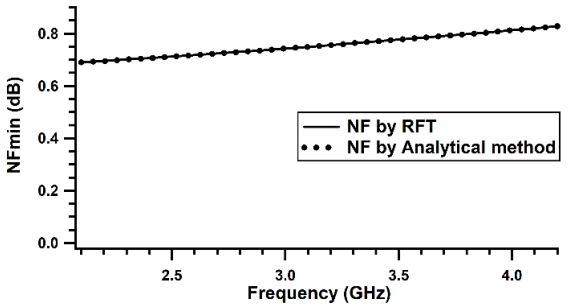

(b)

Fig. 10. The Comparison between the performance of the proposed broadband LNA by RFT and Analytical method. (a) Gain (dB) and (b) NFmin (dB).

TABLE III: COMPARISON OF THE PREVIOUS DESIGNS OF LNA

Ref.	Frequency range (GHz)	Fractional BW (%)	NF (dB)	Gain (dB)	Gain Flatness (dB)	Matching Technique
This work	**2.1-4.2**	**66.67**	**0.69-0.83**	**19.2**	**±0.2**	**RFT**
[23]	1.7-2.3	30	0.62-0.69	17.8	±0.65	compensated matching network
[24]	8–16	66.67	<1	11.5	± 0.2	Modified compensated matching
[25]	6.5-12	59.4	3.26	20.2	±0.5	A frequency-selective non-foster gain equalization
[26]	4-8	66.6	1.5	18	±0.6	RLC feedback
[27]	0.4 -0.8	66.67	1	25.7	±0.65	Shunt negative feedback
[28]	3-5	50	<2.4	14	±0.2	Negative feedback
[29]	1.6 -2.4	40	1.5	18	<1	RLC feedback
[30]	2-4	66.67	<1.25	27	±0.5	Negative-feedback circuit and equalizer heory

Table III depicts the performance of the proposed broadband LNA circuit compared to several previously mentioned ones. The comparison has shown outstanding performance of the proposed designed LNA. Furthermore, the proposed RFT approach is useful for designing broadband LNA with high flat gain while maintaining the NF as low as possible.

IV. CONCLUSION

Based on the new proposed approach of RFT for the designing of broadband LNA and broadband matching theory, LNA has been designed by using ADS and MATLAB platform. Moreover, the matching networks are composed of second-order LC lumped elements to expand the bandwidth and gain flatness of LNA while maintaining low NF. The design result verifies the effectiveness of this approach in a gain of 19.19 dB with ±0.2gain flatness. Besides, the proposed method results have been compared with an analytical methodology that has exhibited a gain of 18.29 dB with an associated ripple of ±0.4dB. Meanwhile, the NF is less than 1dB throughout over 2.1-4.2 GHz.

ACKNOWLEDGMENT

The author R.M. would like to express her deep thanks for Rokaya Osama, research assistant at photometry dept., National Institute for Standards for her precious discussions and support.

Conflict of Interest

The authors declare no conflict of interest.

Author Contributions

Reham Magdy, Gehan S. Shehata, Mahmoud A. Mohanna conducted the research; Reham Magdy, Gehan S. Shehata, Ahmed S. I. Amar analyzed the data and provided the corresponding interpretations; Reham Magdy, Gehan S. Shehata, Ahmed S. I. Amar wrote the paper; Mahmoud A. Mohanna and M. ElHawary reviewed the paper, all authors worked on the concept, and literature survey and approved the final version.

References

[1] N. Gao-Li, Z. Y. Lei, L. J. Zhang, R. Zou, and L. Shao, "Design of concurrent low-noise amplifier for multi-band applications," *Progress in Electromagnetics Research C*, vol. 22, pp. 165-178, 2011.

[2] C. Wang, *et al*., "Cellular architecture and key technologies for 5G wireless communication networks," *IEEE Communications Magazine*, vol. 52, no. 2, pp. 122-130, 2014.

[3] A. Amin, M. Islam, A. Masud, and M. Khan, "Design and performance analysis of 1.8 GHz low noise amplifier for wireless receiver application," *Indonesian Journal of Electrical Engineering and Computer Science*, vol. 6, no. 3, pp. 656-626, 2017.

[4] H. Yu-Chih, M. Chinchun, and L. Meng-Che, "Analysis and design of broadband LC-ladder FET LNAs using noise match network," *IEEE Trans. Microw. Theory Tech.*, vol. 66, no. 2, pp. 987-1001, 2018.

[5] D. Barras, F. Ellinger, and H. Jackel, "A comparison between ultra-wideband and narrow-band transceivers," *TRLabs/IEEE Wireless*, pp. 211–214, 2002.

[6] A. Grebennikov, N. Kumar, and B. S. Yarman, Broadband RF and Microwave Amplifiers, 2015.

[7] D. M. Pozar, *Microwave Engineering*. 4th ed., New York: Wiley, 2012.

[8] N. D. Ahmad, A. Lutfi, and A. Hani, "An overview of design techniques for high frequency wideband low noise amplifiers," in *Proc. IEEE Symposium on Computer Applications & Industrial Electronics*, Penang Island, Malaysia, April 2018, pp. 139-144.

[9] H. Zhou, *et al*., "Analysis and design of a 3.1–10.6 GHz wideband low-noise amplifier using resistive feedback," in *Proc. IEEE International Conference on Ubiquitous Wireless Broadband (ICUWB)*, Nanjing, China, October 2016, pp. 1-3.

[10] T. Cappello, P. Pednekar, C. Florian, S. Cripps, Z. Popovic, and T. W. Barton, "Supply- and load-modulated balanced amplifier for efficient broadband 5G base stations," *IEEE Trans. Microw. Theory Tech.*, vol. 67, no. 7, pp. 3122–33, 2019.

[11] S. Wang and B. Z. Huang, "A high-gain CMOS LNA for 2.4/5.2-GHz WLAN applications," *Progress In Electromagnetics Research C*, vol. 21, pp. 155-167, 2011.

[12] S. Mohadeskasaei, J. An, Y. Chen, Z. Li, S. Abdullahi, and T. Sun, "Systematic approach for design of broadband, high efficiency, high power RF amplifiers," *ETRI Journal*, vol. 39, no. 1, pp. 51-61, 2017.

[13] K. Sedat and B. S. Yarman, "A novel method to design broadband flat gain and sufficiently efficient power amplifiers using real frequency technique," in *Proc. IEEE International Conference on Electronics, Circuits, and Systems(ICECS)*, Batumi, Georgia, December 2017.

[14] N. Poluri and M. D. Souza, "Designing a broadband amplifier without load–pull," *IEEE Microwave and Wireless Components Letters*, vol. 31, no. 6, pp. 593-596, 2021.

[15] NPN Wideband Silicon Germanium RF Transistor, BFU730F, NXP, Netherlands, April 2011.

[16] N. Sadia and H. Mehmood, "Stabilization of microwave amplifiers," in *Proc. Pakistan Section Multitopic Conference. IEEE*, Karachi, Pakistan, December 2005.

[17] W. Fei and T. Chau, "A generic broadband matching network synthesizer using real frequency technique," *International Journal of RF and Microwave Computer-Aided Engineering*, vol. 28, no. 4, p. e21227, 2018.

[18] B. S. Yarman, *Design of Ultra Wideband Power Transfer Networks via Real Frequency Techniques*, Willey, UK., 2010.

[19] G. Gonzalez, *Microwave Transistor Amplifiers: Analysis and Design*, Prentice-Hall, NJ, USA, 1997.

[20] H. Carlin and B. Yarman, "The double matching problem: Analytic and real frequency solutions," *IEEE Transactions on Circuits and Systems*, vol. 30, no. 1, pp. 15-28, 1983.

[21] T. H. Tri, *Solid-state Microwave Amplifier Design*, New York, 1981.

[22] J. M. Douglas, "Improved computer-aided synthesis tools for the design of matching networks for wideband microwave amplifiers," *IEEE Trans. Microw. Theory Tech.*, vol. 34, no. 12, pp. 1276-1281, 1986.

[23] M. A. Ahmed, *et al*., "Design and implementation of a broadband high gain low noise amplifier for 3G/4G applications," *Indonesian Journal of Electrical Engineering and Computer Science*., vol. 23, no. 2, pp. 725-732, 2021.

[24] M. S. Morteza, "A new design approach of low-noise stable broadband microwave amplifier using hybrid optimization method," *IETE Journal of Research*, pp. 1-7, 2020.

[25] H. Gao, N. Li, M. Li, *et al*., "A 6.5-12 GHz balanced variable gain low-noise amplifier with frequency-selective non-foster gain equalization technique," in *Proc. IEEE/MTT-S International Microwave Symposium (IMS)*, Los Angeles, United States, August 2020, pp. 321-324.

[26] C. Chen, *et al*., "A wideband low noise flat gain amplifier for interferometric passive microwave imaging system," in *Proc. PhotonIcs & Electromagnetics Research Symposium-Spring (PIERS-Spring)*, Rome, Italy, June 2019, pp. 3526-3529.

[27] W. Ittaboon and P. Janpugdee, "A UHF broadband low-noise amplifier for active digital TV antenna," in *Proc. 34th International Technical Conference on Circuits/Systems,*

Computers and Communications, Jeju, South Korea, June 2019, pp. 1-4.
[28] P. Gámez, A. Altieri, and C. Galarza, "High gain flatness discrete low noise amplifier for 3 to 5 GHz UWB operation," in *Proc. Argentine Conference on Electronics (CAE)*, Mar del Plata, Argentina, March 2019, pp. 65-69.
[29] L. Jing and B. N. Gao, "Design of 1.6-2.4 GHz low noise amplifier based on SiGe HBT," in *Proc. IEEE International Conference on Electron Devices and Solid-State Circuits (EDSSC)*, Xi'an, China, June 2019, pp. 1-3.
[30] Q. Xiao-Dong, Y. Li, and M. H. Fu, "Design of broadband low noise amplifier with high gain and high flatness," in *Proc. International Conference on Microwave and Millimeter Wave Technology*, Chengdu, China, May 2018, pp. 1-3.

Reham Magdy is a Research Assistant with the Time, Frequency and Microwave laboratory in National Institute of Standards (NIS), Egypt. She received B.S. degree in electrical engineering from Benha University, Shoubra Faculty of Engineering, Cairo, in the current state she is M.Sc. degree student in electrical and communication engineering, Shoubra Faculty of Engineering.

Gehan S. Shehata was born in Cairo, Egypt, in 1976. She received B.SC. degree in electrical engineering from Benha University, Shoubra Faculty of Engineering, Cairo, 1999, and the M.SC. and Ph.D. degrees in electrical engineering from Benha University of Engineering, in 2005 and 2013, respectively. Since 2013, she has joined the Department of Electrical Engineering, Shoubra Faculty of Engineering, as a lecturer. Her current interest areas of research are broadband microwave circuit design, microwave imaging, and broadband antennas for ground penetrating radar.

Ahmed S. I. Amar received the B.S. degree in electrical engineering from the University of Alexandria, Alexandria, Egypt, in 2008, and the M.Sc. degree in electrical engineering from the Ain Shams University, Cairo, Egypt, in 2016. He is currently an Assistant Researcher at Electromagnetic Fields Department, ADR&D Center, Egypt, and aiming for getting a Ph.D. degree from Ain Shams University. His current research interests include Antennas, RF and Microwave Circuit Design, Power Amplifiers, and Millimeter-wave passive and active circuits Design.

Mohamed El Hawary is a researcher in the National Institute of Standards (NIS), Egypt. He received his Ph.D. and M.Sc. degrees in Communications and Electronics from Faculty of Engineering, Ain Shams University, Egypt. His research interests include GNSS receivers, time and frequency dissemination through using GPS receivers and FPGA.

Mahnoud A. Mohanna received B.Sc. with honored degree from faculty of engineering, Cairo University Egypt, in 1968. He worked as radar specialist in Air defense, in Egypt until 1988, received Ph. D. in electronic engineering in 1994. Joined in Egyptian National Seismic Network 1995, NRIAG, EGYPT. Tenured Prof. in NRIAG from 2006 until now.